DOI: 10.1002/cbic.200800719

A Shielding Topology Stabilizes the Early Stage Protein–Mineral Complexes of Fetuin-A and Calcium Phosphate: A Time-Resolved Small-Angle X-ray Study

Christophe N. Rochette,[a] Sabine Rosenfeldt,[a] Alexander Heiss,[b] Theyencheri Narayanan,[c] Matthias Ballauff,*[a] and Willi Jahnen-Dechent*[b]

We report on the earliest stages of the formation of complexes of calcium phosphate in the presence of the serum protein α_2-HS glycoprotein/fetuin-A termed calciprotein particles (CPPs). Time-resolved small-angle X-ray scattering (TR-SAXS) and stopped-flow analysis were used to monitor the growth of protein mineral particles nucleating from supersaturated salt solutions. It was found that fetuin-A did not influence the formation of mineral nuclei. However, fetuin-A did prevent the aggregation of nuclei and thus mineral precipitation. Hence, fetuin-A shielded spontaneously formed mineral nuclei, leading to stable calciprotein particles in the first stage of mineralization. Fetuin-A is therefore critically required during the earliest stages of the formation of protein–mineral complexes in order to prevent uncontrolled mineralization.

Introduction

Nature controls the crystallization of inorganic materials in a process called biomineralization, resulting in organic–inorganic hybrid materials with unique material properties. Mineralization only occurs under well controlled conditions; otherwise it must be prevented in a suitable way. The handling of calcium phosphate in mammals illustrates an important point: the concentrations of calcium and phosphate ions in mammalian blood are much higher than would be predicted from the solubility product for basic calcium phosphate.[1–4] Calcium phosphate would therefore be expected to precipitate all over the human body, but mineralization is usually restricted to bones and teeth. Recent work has identified the serum protein α_2-HS glycoprotein/fetuin-A as an important inhibitor that prevents pathological mineralization in soft tissues and in the extracellular fluid.[2] The mechanism of this inhibition is related to the formation of the so-called calciprotein particles (CPPs).[3,5–7] Once the solubility product is exceeded by the concentration of Ca^{2+} and phosphate, colloidal CPPs that consist of amorphous calcium phosphate and fetuin-A are formed. In body fluids, acidic proteins such as serum albumin further stabilize the colloid.[7] Studies by transmission electron microscopy (TEM) and dynamic light scattering revealed that CPPs have diameters of the order of 25–150 nm.[3,6,7]

By employing small-angle neutron scattering (SANS) we recently demonstrated that the initial CPPs transform into mature secondary CPPs each consisting of a core of octacalcium phosphate covered by a shell of fetuin-A.[6] The analysis by SANS, however, required at least 30 min per sample, so SANS did not permit the study of early stages of CPP formation, and critical information about the early stages of mineral nucleation and the formation of CPPs in the presence of fetuin-A is still lacking.

We considered two alternative mechanisms of mineralization inhibition in the early stage: 1) fetuin-A could act as a nucleating agent but forming a large number of nuclei onto which the solid mineral precipitates; this would effectively decrease the ion product driving mineral formation, or 2) fetuin-A could shield spontaneously forming mineral nuclei, thus effectively preventing their further growth and ultimately their precipitation. In the first case the number (N) of particles in a given volume (V) should be directly proportional to the fetuin-A concentration. At the same time, the sizes of the primary particles should decrease. If, on the other hand, fetuin-A acted as a surface active component, stabilizing the particles and preventing further growth by aggregation, neither N/V nor the sizes of the primary particles should change markedly in the presence of fetuin-A.

Here we present a detailed study of the early stage of the CPP formation based on time-resolved small-angle X-ray scattering (TR-SAXS). Calcium ions and phosphate ions were mixed rapidly in a stopped-flow apparatus and the growth of mineral particles was monitored through the increase and angular dependence of the scattering intensity. As shown previously, the number density (N/V) and particle radius (R) can be extracted from TR-SAXS data.[8–10] Measurements were taken without and with fetuin-A, and the role of this protein in the early stage of mineralization was assessed. Together with previous data relat-

[a] C. N. Rochette, Dr. S. Rosenfeldt, Prof. Dr. M. Ballauff
Physikalische Chemie I, University of Bayreuth
95444 Bayreuth (Germany)
Fax: (+49) 921-55-2780
E-mail: matthias.ballauff@uni-bayreuth.de

[b] Dr. A. Heiss, Prof. Dr. W. Jahnen-Dechent
Department of Biomedical Engineering-Biointerface Group
RWTH Aachen University
52074 Aachen (Germany)

[c] Dr. T. Narayanan
European Synchrotron Radiation Facility
38043 Grenoble Cedex (France)

 © 2009 Wiley-VCH Verlag GmbH & Co. KGaA, Weinheim

ing to longer timescales[3,6,7] our present study provides a complete time-resolved mechanism of the formation, maturation and stability of CPPs.

Results and Discussion

In order to study the effect of the glycoprotein on the formation of calcium phosphate complexes, we first performed measurements in the absence of fetuin-A. Solutions of 20 mM Ca^{2+} and 12 mM PO_4^{3-} were prepared with a buffered solution (pH 7.4). The concentrations of Ca^{2+} and PO_4^{3-} solutions were thus chosen in order to match the experimental conditions used in our previous SANS study.[5] Figure 1 shows the normalized SAXS intensities up to $t = 1.355$ s. Here and in all subsequent scattering curves the background has been subtracted. Except for a small minimum around 0.28 nm^{-1}, the decay of the scattering intensity does not exhibit any pronounced minima or maxima. However, a pronounced upturn of the scattering intensity is observed at the smallest q vectors ($q < 0.15$ nm^{-1}). No change in the scattering intensity is observed after about 0.255 s. We found that the scattering patterns recorded at later time points (145 s after the mixing process; data not shown) were similar to those at 0.26 s. In general, the intensities measured at intermediate and high q ranges virtually agree beyond 250 ms and only differ in the region of small q values. Moreover, no shift of the minimum was observed any longer, indicating that the formation of particles had completed.

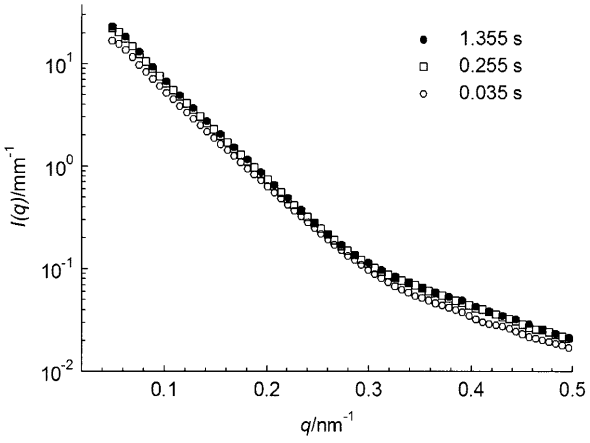

Figure 1. Evolution of the normalized SAXS intensities in the absence of fetuin-A. Later SAXS intensities did not show any evolution of the shape or the intensity. This demonstrates the very fast kinetics of early calcification leading to the first equilibrium phase of Ca_3PO_4 particles. For the sake of clarity only every second point is shown for the intensity measured after 1.355 s. Concentrations: Ca^{2+} (10 mM) and PO_4^{3-} (6 mM) in Tris/HCl buffer (50 mM).

Evidently, the formation of primary particles of calcium phosphate is very fast. After this stage aggregation sets in, leading to the upturn at small q values. Obviously, aggregation is beginning at a very early stage, directly after the formation of the primary particles. A similar observation has been made in a recent study of the formation of $CaCO_3$ particles.[8]

To study the effect of fetuin-A, the measurements were repeated under the same experimental conditions in the presence of 1, 5 and 15 μM fetuin-A, the last of these corresponding to its physiological concentration in plasma. The solubility product (K_{sp}) for amorphous calcium phosphate at the given pH and temperature is estimated as $10^{-25.7}$.[11] Thus, the mineral ion concentrations used here (i.e., supersaturation) greatly exceeded their physiological serum concentrations. We reasoned, however, that local concentrations—within the skeleton, for example—might be much higher and should still be effectively controlled by fetuin-A.

The evolution of the SAXS intensities as a function of time is displayed in Figure 2 for the sample containing fetuin-A (15 μM). A slight shoulder is evident. Moreover, the absolute scale and the upturn of the scattering intensity at the lowest q values was lower than without fetuin-A (Figure 1). We conclude that the presence of fetuin-A led to much smaller mineral particles.

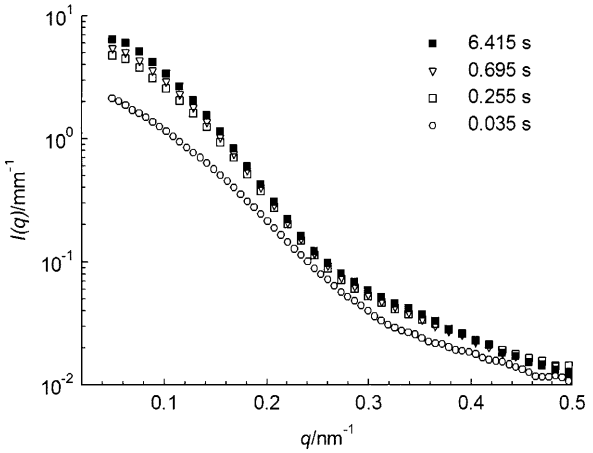

Figure 2. Evolution of the normalized SAXS intensities with time in the presence of fetuin-A (15 μM). SAXS intensities measured at longer times did not show any change either in the shape or in intensities. Here we note slower formation of the primary spherical particles than in the sample without fetuin-A (Figure 1). For the sake of clarity only every second point is shown for the upper curves. Concentrations: Ca^{2+} (10 mM) and PO_4^{3-} (6 mM) in Tris/HCl buffer (50 mM).

Figures 3 and 4 present a typical analysis of SAXS intensities made with the aid of Equation (6) at the times indicated. The smeared side maximum of $I(q)$ indicated polydispersity of the particles. In the region of the smallest q values we find that data obtained without fetuin-A or at low concentrations thereof cannot be fitted by assuming a solution of non-interacting spheres (that is, by assuming $S(q) \approx 1$ in Equation (6), below; see Modelling). In these cases the deviation at small q values indicated aggregation of mineral nuclei as already discussed in conjunction with Figures 1 and 2. The resulting scattering intensities were therefore modelled as a system of aggregated spheres (that is, by use of the structure factor $S(q)$ given in Equation (4), below). At elevated fetuin-A concentrations (for

 © 2009 Wiley-VCH Verlag GmbH & Co. KGaA, Weinheim

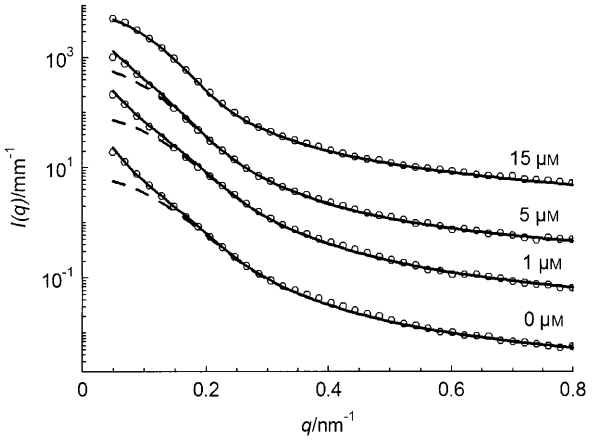

Figure 3. Normalized SAXS intensities 0.23 s after the mixing process. The figure shows (from bottom to top) the scattering intensities of the samples containing 0, 1, 5 and 15 μM of fetuin-A. For the sake of clarity, intensities were multiplied by factors of 10 (1 μM), 100 (5 μM) and 1000 (15 μM). For fitting of the sample with the highest concentration of fetuin-A (15 μM), $S(q)$ was assumed to be unity (that is, no aggregation took place under these conditions). For all other concentrations aggregation was taken into account by assuming $S(q) > 1$ [Eq. (6)]. For the sake of clarity only every third point of the experimental data is shown. Concentrations: Ca^{2+} (10 mM) and PO_4^{3-} (6 mM) in Tris/HCl buffer (50 mM).

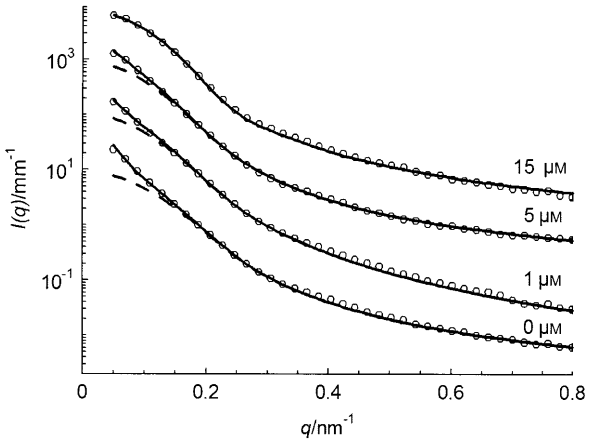

Figure 4. Modelling of the normalized SAXS intensities 0.89 s after the mixing process. The figure shows (from bottom to top) the scattering intensities of the samples containing 0, 1, 5 and 15 μM of fetuin-A. For the sake of clarity, intensities were multiplied by factors of 10 (1 μM), 100 (5 μM) and 1000 (15 μM). For fitting of the sample with the highest concentration of fetuin-A (15 μM), $S(q)$ was assumed to be unity (that is, no aggregation took place under these conditions). For all other concentrations aggregation was taken into account by assuming $S(q) > 1$ [Eq. (6)]. For the sake of clarity only every third point of the experimental data is shown. Concentrations: Ca^{2+} (10 mM) and PO_4^{3-} (6 mM) in Tris/HCl buffer (50 mM).

example, 15 μM), aggregation of primary particles was absent. Hence, under these conditions the protein molecules seem to cover each spherical particle completely and thus prevent further aggregation.

The fits shown in Figures 3 and 4 allowed us to derive the parameters of number density (number of particles over volume, N/V) and radii of the primary particles (R_{psp}) as a function of time as given in Equation (3), below. Both quantities were subject to considerable error because the polydispersity of the primary particles was high. Polydispersity was taken into account by use of a distribution function for the radii. With a Gaussian distribution function the deviations of the radii from the radius of the mean particle were in the 20–55% range, depending on time and amount of fetuin-A. Model calculations using different distribution functions (such as Schulz–Zimm) led to slight changes in the absolute values of N/V and R_i and the corresponding errors. Nevertheless, these calculations gave similar results, so the data sufficed for observation of the general trends. Further evaluation was carried out by use of the mean values obtained from the fits made with a Gaussian distribution function. Figures 5 and 6 demonstrate that both N/V and R_{psp} increased with time but levelled off after less than

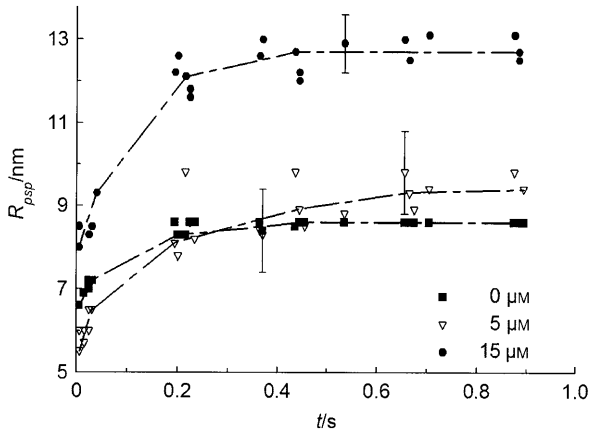

Figure 5. Time-evolution of the radii of primary spherical particles in the absence (■) and in the presence of fetuin-A (▽, ●). Data for fetuin-A (1 μM) were intermediate between those for 0 and 5 μM, but are omitted from the graph for the sake of clarity. The dashed lines describe the general trend of the evolution of the radii of primary spherical particles (R_{psp}). We note here, within the limits of error, growth of the primary particles with the addition of the glycoprotein.

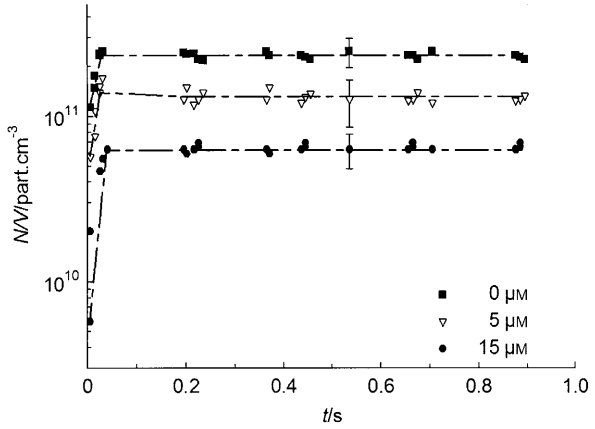

Figure 6. Time-evolution of the number density. Data for fetuin-A (1 μM) were intermediate between those for 0 and 5 μM, but are omitted from the graph for the sake of clarity. The dashed lines describe the general trend of the evolution of the number of particles per volume. We note here, within the limits of error, a decrease in the number of particles per unit volume with the addition of the glycoprotein.

 © 2009 Wiley-VCH Verlag GmbH & Co. KGaA, Weinheim

0.1 s. The error bars give an indication of the range of the mean values obtained by fitting of all data series. The number density increased by an order of magnitude at this very early stage. The exceedingly fast increases both in N/V and in R_{psp} suggested that the primary particles form within a fraction of a second.

This corroborates the results presented here: namely a strongly increased colloidal stability of the CPP by fetuin-A. The particles aggregate much more rapidly if less fetuin-A is in the system.

Moreover, Figures 5 and 6 show that the presence of fetuin-A leads to the formation of larger primary particles but with a smaller number density. From 0 up to 5 μM fetuin-A, no significant differences in growth parameters could be found. Data obtained in the presence of the physiological concentration of fetuin-A (15 μM), however, clearly showed that the number density (N/V) of the primary particles had not increased in the presence of the protein. As already discussed in the Introduction, a nucleation agent would lead to a much increased N/V value. The number density (N/V) had even decreased with increasing fetuin-A concentration. Moreover, we found that within the experimental error, the rate of formation of calcium phosphate did not depend on the concentration of fetuin-A in the solution. This may be directly inferred from plots of $N/V \cdot R_{psp}^3$ versus time t (data not shown). This quantity was proportional to the entire amount of material produced as a function of time t. The error bar of this product was rather high (about 20%) but there was no significant deviation between curves measured for different fetuin-A concentrations. We hence conclude that fetuin-A is not acting here as a nucleating agent. The small changes in N/V and R_{psp} point to only a small effect of the protein on the growth process at a very early stage of CPP formation.

Figure 7 illustrates the aggregation of primary particles in the presence of different amounts of fetuin-A in a quantitative manner. The quantity $S(0)+1$ represents the number of primary particles per aggregate. As demonstrated in Figure 7, no aggregation was observed in solutions containing 15 μM fetuin-A. This is similar to our recent findings on the mineralization of calcium carbonate in the presence of water-soluble block copolymers,[8] which likewise suppressed aggregation of primary mineral particles. The water-soluble block copolymer attached to the surfaces of the particles, thus preventing further aggregation. The same conclusion may be drawn here as well: fetuin-A acts as a surface-active agent that attaches to the surfaces of the amorphous particles of calcium phosphate to provide colloidal stability against coagulation.

Figure 8 summarizes the results obtained by TR-SAXS. The particles monitored in the very early stage in the TR-SAXS experiment consist of amorphous calcium phosphate stabilized by a surface layer of fetuin-A. The surface layer of fetuin-A protein positively identified in our recent SANS experiment[5] could not be resolved by SAXS due to a lack of contrast (see the Experimental Section). However, the assumption of a stabilizing surface layer is in full agreement with previous studies by DLS and SANS.[6,7] We can now specify that "inhibition" of mineralization by fetuin-A operates through stabilization of the primary particles against coagulation rather than through prevention of mineralization altogether. Once the concentrations of the ions exceed the solubility product, the primary particles must precipitate. The process of precipitation is fast (< 0.1 s) and fetuin-A has little influence at this very early stage. However, aggregation of these primary particles, with sizes in colloidal dimensions, commences immediately thereafter. At this stage fetuin-A can intervene by stabilizing the primary particles through formation of the CPPs. These particles are remarkably stable against further aggregation.

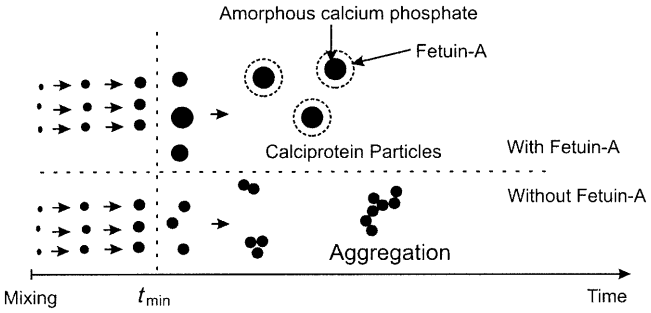

Figure 8. Role of fetuin-A in the early stage of mineralization. Calcium phosphate particles are generated once the concentrations of the ions exceed the solubility product. Virtually no influence of fetuin-A that cannot be studied by the present experimental setup is seen in this early stage. The primary particles are then stabilized by the protein through the formation of the calciprotein particles. Without fetuin-A, large aggregates are formed.

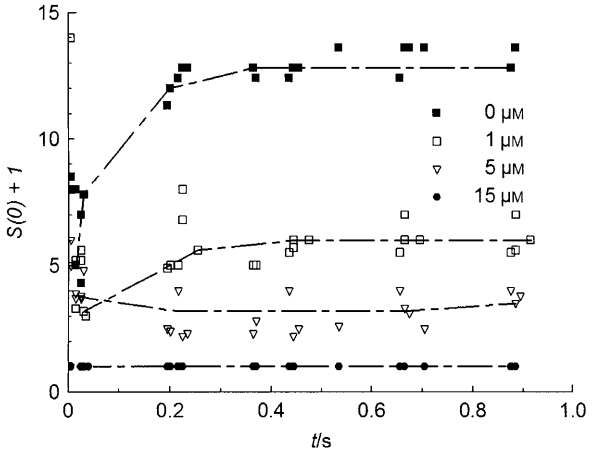

Figure 7. Time-evolution of the average number of primary particles per aggregate. As noted previously (Figures 3 and 4), no structure factor was used for fitting SAXS data for the sample containing fetuin-A (15 μM) [$S(0)+1=1$]. The number of primary particles per aggregate decreases with the addition of glycoprotein, demonstrating the inhibitor effect of the glycoprotein on calcification. The dashed lines represent the general trend of the evolution of the number of primary particles per aggregate.

In conclusion, we present a time-resolved synchrotron SAXS study detailing the formation of calcium phosphate complexes with the plasma protein fetuin-A. The most significant effect observed was that fetuin-A stabilized the mineral particles,

 © 2009 Wiley-VCH Verlag GmbH & Co. KGaA, Weinheim

preventing their subsequent aggregation if the protein was present in sufficient concentration. The calciprotein particles thus formed exhibited remarkable long-term stability.[7]

Experimental Section

CPP preparation: Calcium chloride ($CaCl_2 \cdot 2H_2O$, Roth GmbH, Karlsruhe) and sodium phosphate ($Na_3PO_4 \cdot 12H_2O$, Fluka) were analytical grade. Solutions of Ca^{2+} (20 mM) and PO_4^{3-} (12 mM) were prepared with a buffered solution (50 mM Tris/HCl, AppliChem, Darmstadt, pH 7.4). The concentrations of Ca^{2+} and PO_4^{3-} solutions were chosen in order to match the experimental conditions used in our previous SANS study.[5] Commercial bovine fetuin-A was purified as described previously.[3] The glycoprotein was diluted into the calcium and phosphate solutions at concentrations of 0, 1, 5 and 15 μM.

All TR-SAXS experiments were performed at the high-brilliance undulator beamline ID2 at the ESRF, Grenoble, France.[12] The wavelength (λ) of radiation was chosen as 1 Å. The SAXS patterns were recorded with a high-sensitivity fibre-optically coupled CCD detector (FReLoN). The sample-to-detector distance was set to 2 m. Data acquisition and counting of the time t was hardware-triggered within 1 ms before the final mixing process was initiated. SAXS data were acquired in increments of 170–520 ms with an exposure time of 20–50 ms per frame. By repetition of the experiment with different initial delay times the time intervals between the readout gap of the detector (about 80 ms) could, when required, be interpolated to achieve better time resolution. In this way the reaction was followed during the first 8 s after mixing.

Rapid and effective mixing of the $CaCl_2 \cdot 2H_2O$ and $Na_3PO_4 \cdot 12H_2O$ solutions was accomplished at 37 °C by use of a stopped-flow device (BioLogic SFM-3), leading to Ca^{2+} (10 mM) and PO_4^{3-} (6 mM) after the mixing (ratio 1:1). The mixing volumes and the mixer flow rates were controlled with the instrument software. The total mixer flow rate and the capillary during the final mixing phase were set to an optimum value of 6.67 mL s^{-1}. After 30 ms of continuous mixing and flowing through the capillary, the flow of the reagent mixture through the capillary was stopped and the sample was left unperturbed. The kinetic time evolved above the dead time of the device (~4 ms: that is, the time needed to transfer the mixture to the point of measurement in the capillary) after the cessation of the flow. Thus for times $t \leq 35$ ms there are quasi-steady-state conditions due to the continuous flow of the reaction mixture. The stopped-flow cell filled with the buffer was taken as the background.

Modelling: This analysis of the mineralization by TR-SAXS has been described in detail previously.[8–10] In short, the scattering intensity [$I(q)$] of a system of noninteracting spherical particles can be calculated from Equation (1):[13]

$$I(q) = \sum_i \frac{N_i}{V} B_i^2(q) \quad (1)$$

where the index i refers to the fraction of particles of radius R_i and with a particle number density N_i/V. The scattering amplitude $B_i(q)$ is given by:

$$B_i(q) = 4\pi \int_0^{R_i} [\rho(r) - \rho_m] \frac{\sin(qr)}{qr} r^2 dr \quad (2)$$

where ρ and ρ_m represent the electron contrast of the particles studied and of the solvent, respectively.

For homogeneous spheres, $I(q)$ is given by:

$$I(q) = \sum_i \frac{N_i}{V} (\rho - \rho_m)^2 V_i^2 \left(3 \frac{\sin(qR_i) - qR_i \cos(qR_i)}{(qR_i)^3}\right)^2 \quad (3)$$

with V_i representing the volume per particle. The assumption of a spherical shape of the CPP was derived from our previous work[3] showing that the CPPs have a spherical shape in the earliest stage. Polydispersity was accounted for by assuming a normalized Gaussian number distribution.

Interparticle interaction and aggregation were both accounted for with a structure factor $S(q)$. The effect of $S(q)$ is restricted to the smallest q region in which a length scale of interparticle distances is being probed. Fractal aggregation of the primary particles can be modelled by the following expression for $S(q)$:[14]

$$S(q) = 1 + \frac{S(0)}{[1 + q^2\xi^2]^{(D-1)/2}} \frac{\sin[(D-1)\tan^{-1}(q\zeta)]}{(D-1)q\zeta} \quad (4)$$

where D is the fractal dimension and ζ is a crossover length that is a measure of the aggregate size. The average number of primary particles per aggregate is given by $1 + S(0)$.

Scattering contributions in high-q regions due to density fluctuations within the particles may be described by an additive Ornstein–Zernike term [Eq. (5)]:[10]

$$I_{fluc}(q) = \frac{I_{fluc}(0)}{1 + \xi^2 q^2} \quad (5)$$

where ξ is the average correlation length, which is of the order of a few nanometers.

Thus, the overall theoretical intensity $I_{tot}(q)$ is given by:

$$I_{tot}(q) = S(q)[I(q) + I_{fluc}(q)] \quad (6)$$

The electron density (ρ) of a particle is directly proportional to its mass density (ρ_T). From the mass density and the chemical composition, the electron density can be calculated. The density (ρ_T) of the calciprotein particles was determined through densitometry (DMA 60/602, Paar, Graz, Austria) to be 1.72 g cm^{-3}. WAXS experiments performed on particles obtained with and without fetuin-A (data not shown) did not exhibit any Bragg peaks indicative of crystalline phases. Therefore we concluded that the particles formed in the early stage were amorphous. This is in agreement with previous work[6] demonstrating that an amorphous precursor phase of calcium phosphate is formed first. Similar findings have been reported for the early stage of the formation of calcium carbonate particles.[8–10] The nucleation of the amorphous phase is a fast process and the formation of crystalline modifications follows at a later stage.

The chemical composition of amorphous calcium phosphate (ACP) is not known precisely.[11,15–20] We approximated the contrast of ACP by taking the average of the densities of crystalline tricalcium phosphate (TCP, $Ca_3(PO_4)_2$, $\rho_T = 2.89$ g cm^{-3}, $\rho = 864$ e nm^{-3}) and water (H_2O, $\rho_T = 1.00$ g cm^{-3}, $\rho = 334$ e nm^3). By comparison of the density (ρ_T) of the calciprotein particles with the density and the electron contrast of crystalline TCP, the electron density of ACP was estimated to be $\rho = 536$ e nm^{-3}. As stated above, the contrast of the particles is given by the excess electron density (that is, the

 © 2009 Wiley-VCH Verlag GmbH & Co. KGaA, Weinheim

difference of the average electron density within particles and the corresponding value of the water solvent). For the CPPs this contrast was very high (202 e nm^3). The excess electron contrast of the fetuin-A glycoprotein was determined to be 74 e nm^{-3} (1.32 g cm^{-3} and 50.09 kDa by analytical ultracentrifugation).[5] Therefore, minor differences in the electron density within the particles—through, for example, preferred localisation of the protein on the surface of the particles—should go unnoticed when intensity is measured. The CPPs were therefore treated as homogeneous spheres.[8]

Acknowledgements

We gratefully acknowledge the European Synchrotron Radiation Facility (Grenoble, France) for the provision of synchrotron beam time (SC1652, SC2029) and the German Research Foundation (Deutsche Forschungsgemeinschaft, priority program "Principles of Biomineralization") and the Marie Curie Research and Training Network (Polyamphi) for financial support.

Keywords: aggregation · biomineralization · calciprotein particles · fetuin-A · small-angle X-ray scattering (SAXS)

[1] C. Schäfer, W. Jahnen-Dechent in *Handbook of Biomineralization* (Eds.: E. Baeuerlein, P. Behrens, M. Epple), Wiley-VCH, Weinheim, **2007**, pp. 317–327.
[2] C. Schäfer, A. Heiss, A. Schwarz, R. Westenfeld, M. Ketteler, J. Floege, W. Müller-Esterl, T. Schinke, W. Jahnen-Dechent, *J. Clin. Invest.* **2003**, *112*, 357–366.
[3] A. Heiss, A. DuChesne, B. Denecke, J. Grötzinger, K. Yamamoto, T. Renné, W. Jahnen-Dechent, *J. Biol. Chem.* **2003**, *278*, 13333–133411.
[4] P. A. Price, G. R. Thomas, A. W. Pardini, W. F. Figueira, J. M. Caputo, M. K. Williamson, *J. Biol. Chem.* **2002**, *277*, 3926–3934.
[5] A. Heiss, W. Jahnen-Dechent, H. Endo, D. Schwahn, *Biointerphases* **2007**, *2*, 16–20.
[6] A. Heiss, D. Schwahn in *Handbook of Biomineralization* (Eds.: E. Baeuerlein, P. Behrens, M. Epple), Wiley-VCH, Weinheim, **2007**, pp. 415–431.
[7] A. Heiss, T. Eckert, A. Aretz, W. Richtering, W. van Dorp, C. Schäfer, W. Jahnen-Dechent, *J. Biol. Chem.* **2008**, *283*, 14815–14825.
[8] J. Bolze, D. Pontoni, M. Ballauff, T. Narayanan, H. Cölfen, *J. Colloid Interface Sci.* **2004**, *277*, 84–94.
[9] J. Bolze, B. Peng, N. Dingenouts, T. Narayanan, M. Ballauff, *Langmuir* **2002**, *18*, 8364–8369.
[10] D. Pontoni, J. Bolze, N. Dingenouts, T. Narayanan, M. Ballauff, *J. Phys. Chem. B* **2003**, *107*, 5123–5125.
[11] S. V. Dorozhkin, M. Epple, *Angew. Chem.* **2002**, *114*, 3260–3277; *Angew. Chem. Int. Ed.* **2002**, *41*, 3130–3146.
[12] T. Narayanan, O. Diat, P. Bösecke, *Nucl. Instrum. Methods Phys. Res., Sect. A* **2001**, *1005*, 467–468.
[13] A. Guinier, J. Fournet, *Small Angle Scattering of X-rays*, Chapman & Hall, London, **1955**.
[14] H. Hoekstra, J. Mewis, T. Narayanan, J. Vermant, *Langmuir* **2005**, *21*, 11017–11025.
[15] J. D. Termine, A. S. Posner, *Arch. Biochem. Biophys.* **1970**, *140*, 307–317.
[16] R. E. Wuthier, G. S. Rice, J. E. B. Wallace, R. L. Weaver, R. Z. LeGeros, E. D. Eanes, *Calcif. Tissue Int.* **1985**, *37*, 401–410.
[17] H. E. Lundager Madsen, I. Lopez-Valero, V. Lopez-Acevedo, R. Boistelle, *J. Cryst. Growth* **1986**, *75*, 429–434.
[18] J. Christoffersen, M. R. Christoffersen, W. Kibalczyc, F. A. Andersen, *J. Cryst. Growth* **1989**, *94*, 767–777.
[19] M. S. Johnsson, G. H. Nancollas, *Crit. Rev. Oral Biol. Med.* **1992**, *3*, 61–82.
[20] J. L. Meyer, E. D. Eanes, *Calc. Tissue Res.* **1978**, *25*, 59–68.

Received: November 3, 2008
Published online on February 16, 2009

 © 2009 Wiley-VCH Verlag GmbH & Co. KGaA, Weinheim